Flow Synthesis of Plasmonic Gold Nanoshells via a Microreactor

Satoshi Watanabe[*]*, Tatsumasa Hiratsuka, Yusuke Asahi, Asumi Tanaka, Kazuhiro Mae, and Minoru T. Miyahara*[*]

Department of Chemical Engineering, Kyoto University, Katsura, Nishikyo, Kyoto 615-8510, Japan
E-mails: nabe@cheme.kyoto-u.ac.jp (S.W.); miyahara@cheme.kyoto-u.ac.jp (M.T.M.)

Gold nanoshells with tunable surface plasmon resonances are a promising material for optical and biomedical applications. They are produced through seed-mediated growth, in which gold nanoparticles are seeded on the core particle surface followed by growth of the gold seeds into a shell. However, synthetic gold nanoshell production is typically a multistep, time-consuming batch-type process, and a simple and scalable process remains a challenge. In the present study, a continuous flow process for the seed-mediated growth of silica-gold nanoshells is established by exploiting the excellent mixing performance of a microreactor. In the gold nanoparticle-seeding step, the reduction of gold ions in the presence of core particles in the microreactor enables the one-step flow synthesis of gold-decorated silica particles through heterogeneous nucleation. Flow shell growth is also realized using the microreactor by selecting an appropriate reducing agent. Because self-nucleation in the bulk solution phase is suppressed in the microreactor system, no washing is needed after each step, thus enabling the connection of the microreactors for the seeding and shell growth steps into a sequential flow process to synthesize gold nanoshells. The established system is simple and robust, thus making it a promising technology for producing gold nanoshells in an industrial setting.

1

1. Introduction

In recent years, remarkable progress has been made regarding synthetic techniques for core-shell type functional particles with various combinations of core and shell compositions.[1, 2] Core-shell particles are intriguing because they not only possess varying properties, which is impossible with single-component particles, but they also exhibit peculiar characteristics due to the synergetic effects, interfacial properties, and morphologies of core and shell materials;[3] these characteristics are applicable in a wide range of research fields, including biomedicine,[4] catalysis,[5] optoelectronics,[6] and photovoltaics.[7] Furthermore, plasmonic core-shell particles consisting of metallic (gold or silver) shells on dielectric cores, such as silica or polymer particles, are particularly attractive because of their unique optical and chemical properties, which allow visible and near infrared light to be absorbed and converted into heat with high efficiency, and absorption peaks can be tuned by the ratio of core size to shell thickness. The photothermal conversion characteristics can be advantageous for biomedical applications, such as photoacoustic imaging,[8] photothermal therapy,[9] sensing,[10] and gene silencing,[11] as well as solar energy applications.[12]

The present study focuses on the synthesis of silica-gold core-shell particles (referred to as gold nanoshells). A typical synthetic method is seed-mediated growth, which was originally proposed by Halas and co-workers;[13] this method consists of three steps: surface modification of the core silica particles, gold nanoparticle (AuNP) decoration of the modified silica surface as "seeds," and growth of the AuNP seeds into a shell through the reduction of gold ions. Although this method allows for better control of the shell thickness, the preparation process is rather time consuming, taking days to complete. The bottleneck step is the AuNP seeding process, in which AuNPs are separately prepared by the reduction of gold ions,[14] aged for a certain period, ranging from several days to two weeks,[15] and then mixed with a suspension of surface-modified silica particles to be adsorbed on the modified silica surface due to the electrostatic attraction between the negatively charged AuNPs and the

positively charged modified silica surface. This process is followed by the separation of unattached AuNPs because of the large excess of added AuNPs that increases adsorption on the silica surface. AuNP synthesis and aging are the most time-consuming steps of the seeding process; thus, the processing period can be effectively shortened down to a few hours by modifying the synthetic procedure for the AuNPs,[16] although the seeding process still involves multiple tedious steps. In terms of the throughput and simplicity of the process, a direct seeding approach *via* the *in situ* reduction of gold ions and nucleation at the core particle surface is more desirable for depositing AuNPs onto the core silica particles. However, nucleation and particle growth are often difficult to control precisely with batch-type synthesis because concentration and temperature distribution is generally difficult to avoid. In fact, direct seeding with a batch reaction results in homogeneous nucleation in the bulk solution phase as well as heterogeneous nucleation on the core particle surface, after which separation processes are necessary to remove the free AuNPs.[17] Although pretreatments of the core particle surface to create nucleation sites can facilitate selective deposition on the particle surface, the procedure is complicated, and the resultant deposition tends to be less uniform than that by the adsorption method mentioned above.[18] The shell formation process is also not straightforward because self-nucleation in the bulk phase is difficult to avoid during the shell growth process, similar to AuNP seeding.[19] In addition, shell growth is extremely sensitive to the experimental conditions and procedures; thus, it often suffers from poor reproducibility even though the shell growth technique has been modified and improved in recent years.[19, 20, 21] The complexity and sensitivity encountered in the synthetic process is an obstacle to practical applications of gold nanoshells; thus, a robust and facile synthetic process is required.

An intrinsic problem in synthetic gold nanoshell processes is the non-uniform reaction field provided by the weak mixing intensity of a batch-type reactor, which conversely suggests that a reactor providing a uniform reaction field would enable AuNP seeding and

shell growth to be performed in one step through preferential nucleation and growth on the core particle surface. One promising reaction device is a microreactor with excellent mixing and heat-transfer performance, which can instantaneously provide the appropriate reaction conditions of concentration and temperature with which the heterogeneous nucleation at the interface is promoted while self-nucleation in the bulk phase is suppressed. Another advantage of a microreactor is the establishment of a synthetic flow system, which is suitable for scaling up production.[22] Microfluidic systems have been widely applied to nanoparticle synthesis[23] and have recently been extended to the synthesis of silica-gold core-shell structures. Duraiswamy and Khan pioneered gold shell growth using a segmented microfluidic system in which a gold-seeded silica particle suspension containing a solution of gold ions and a reducing agent was mixed to grow AuNP seeds into a shell.[24] Gomez *et al.* applied a single-phase, non-segmented microreactor for the synthesis of surface-functionalized silica particles, for AuNP seeding by the adsorption method, and for shell growth.[25] Hassan *et al.* prepared SiO_2–Au nanostructures by mixing suspensions of surface-modified fluorescent silica particles and AuNPs in a Y-shaped microreactor, followed by the mixing of a suspension of iron oxide nanoparticles, to produce SiO_2–Au–Fe_2O_3 nanostructures.[26] However, the AuNP seeding process remains problematic in these microfluidic approaches, similar to typical batch-type syntheses, because it relies on the electrostatic adsorption of AuNPs, which requires subsequent removal of unattached particles; thus, AuNP seeding and shell growth must be two independent processes. Establishing a flow seeding process based on a method other than the adsorption method is critical for the sequential flow synthesis of gold nanoshells. However, to the best of our knowledge, no studies have successfully developed such a method to date.

In the present study, we establish a continuous flow process that employs the seed-mediated growth method to synthesize gold nanoshells. We apply a non-segmented single-phase microreactor separately to the AuNP seeding and shell growth processes to realize a

one-step flow synthesis for both processes; then, these two processes are combined into a sequential process by employing flow synthesis. In the AuNP seeding process, *in situ* reduction of gold ions is performed by mixing surface-modified silica particles, gold ions, and reducing agents, and the high mixing intensity provided by the microreactor enables the selective deposition of AuNPs on the core silica particles without the nucleation of AuNPs in the bulk solution phase. In the shell growth process, we mix the as-prepared gold-decorated silica particles with gold ions and reducing agents in the microreactor, demonstrating that the microreactor enables effective shell growth through selection of the appropriate reducing agent with moderate reducing ability. Finally, we combine these two processes into a sequential flow system to achieve, for the first time, the continuous synthesis of gold nanoshells from surface-modified silica particles.

2. Results and Discussion

2.1 One-step flow synthesis of gold-decorated silica particles

We first modified 120-nm-diameter silica particles with 3-aminopropyl trimethoxysilane (APTS) to obtain a positive surface charge. The zeta potential of the surface-modified silica particles (referred to as APTS-SiO$_2$) was measured at +45 mV at pH = 3.2 (see Figure S1, which illustrates the dependence of the zeta potential on pH and elapsed time after the reaction), suggesting successful surface modification. These particles were then used as the core particles. In the AuNP seeding process, as shown in **Figure 1**A, we mixed an APTS-SiO$_2$ suspension containing HAuCl$_4$ in syringe A with a reducing agent solution in syringe B by pumping the two solutions into a microreactor with a two-channel syringe pump at a rate of 10 mL/min. The microreactor we used is a central collision-type microreactor, referred to as a K-M mixer; the microreactor is composed of inlet, mixing, and outlet plates (Figure 1B).[27] The concept of the microreactor is to decrease the diffusion distance by bombarding fluid streams at a single mixing point to break them into micron segments of fluids due to shear

forces acting between colliding fluids, because molecular diffusion generally dominates the mixing. The characteristic mixing time is thus determined by the diffusion time, L^2/D, where L is the size of fluid segments and D is the diffusion coefficient. Assuming, e.g., $L = 1$ μm and $D = 10^{-9}$ m^2/s gives the mixing time on the order of 10^{-3} s. As shown in Figure 1B, each of the two inlet fluids injected into the inlet plate branch off into seven channels with a width of 100 μm, and the separated fluids flow through 14 channels and collide at the center of the mixing plate. The fluids are broken into microsegments *via* shear forces due to the collision break, and subsequent molecular diffusion between fluid segments completes the mixing. We used a strong reducing agent, NaBH$_4$, to exploit the high mixing performance of the microreactor. **Figure 2**A, B presents typical transmission electron microscope (TEM) images of the resultant silica particles after the AuNP seeding process when $R = 0.06$, where R ($\equiv$ Au [g/L]/Silica [g/L]) is defined as the ratio of gold ions to core silica particles. Core silica particles are uniformly decorated with monodispersed AuNPs with a diameter of 3.1±0.7 nm. TEM observations confirmed that no unattached AuNPs were present, indicating that the formation of AuNPs occurred only on the core silica surface. The uniform deposition could be attributed to the high mixing intensity of the microreactor, which offers a homogeneous reaction field around the core silica particles, resulting in preferential nucleation at the solid–liquid interface. We confirmed that resultant gold-decorated silica particles are stably dispersed for weeks. Although typical modification procedures use ethanol as a solvent,[2] we conducted the silica surface modification in an aqueous solution because we confirmed that APTS-SiO$_2$ prepared in ethanol results in less uniform AuNP deposition with lower coverage than when prepared in water (Figure S2). Water-treated APTS-SiO$_2$ is more suitable for direct seeding, likely because the microscopic structure of APTS molecules on the silica surface is different between water- and ethanol-treated APTS-SiO$_2$. Further investigation would be necessary to further elucidate this difference. The reaction with a slower flow rate of 5

mL/min yielded silica particles uniformly decorated with monodispersed AuNPs, similar to those obtained at 10 mL/min (Figure 2C); a further decrease in the flow rate to 2.5 mL/min resulted in the attachment of a number of recognizably larger AuNPs on the core silica particle surface, although the AuNP coverage was nearly uniform among the resultant gold-decorated silica particles (Figure 2D). These results demonstrate that the microreactor with a flow rate of 5 mL/min or greater enables one-step direct AuNP seeding through the reduction of gold ions in the presence of core silica particles. In contrast, a batch reactor and Y-shaped mixer (with an inner diameter of 1.5 mm) with weaker mixing intensity resulted in non-uniform deposition of polydispersed AuNPs on the core silica particles (Figure 2E, F). The difference in the AuNP coverage between individual gold-decorated silica particles is also remarkable; some silica particles are fully decorated, whereas others are completely devoid of decoration. Thus the AuNP seeding through *in-situ* reduction of gold ions requires intensive mixing provided by the microreactor, although batch-type synthesis of uniform gold-decorated silica particles is also possible by applying the adsorption method. To quantitatively evaluate the effect of mixing intensity on the AuNP seeding process, we estimated the characteristic mixing times of different mixing procedures by the Villermaux-Dushman method using the iodide/iodate chemical test reaction[28] and plotted the relationship between mixing time and the average diameter of the AuNPs (see Figure 2G). Whereas mixing process times greater than 10 ms (a microreactor with a flow rate of 2.5 mL/min, a batch reactor, and a Y-shaped mixer) produce AuNPs with a wider size distribution, the microreactor with flow rates of 5 and 10 mL/min yield monodispersed AuNPs with a narrow size distribution, demonstrating that a mixing time on the order of milliseconds is necessary for the uniform preparation of gold-decorated silica particles through *in situ* reduction of gold ions.

Doubling the gold ion concentration with a fixed concentration of APTS-SiO$_2$ (R = 0.12) resulted in deposition of aggregated AuNPs in addition to production of unattached AuNPs, whereas a gold concentration lower than that in Figure 2 produced gold-decorated

particles with lower coverage (Figure S3). However, increasing the core silica concentration and gold ion concentration with a fixed R of 0.06 resulted in the uniform deposition of monodispersed AuNPs on core silica particles without the formation of unattached AuNPs, even at a gold concentration that was eight-fold higher than that in Figure 2 (**Figure 3**A), demonstrating that the gold-to-silica ratio (R) is a key parameter for uniform AuNP seeding. These results suggest that the existence of silica particles, *i.e.*, the solid–liquid interface, suppresses self-nucleation in the bulk solution phase. We confirmed the immediate formation of gold-decorated silica particles after mixing by measuring the time evolution of the extinction spectra of a suspension directly collected from the microreactor outlet (Figure S4A). The results contrast those in the case without core silica particles, in which the extinction spectra of gold nanoparticles grow slowly, on the order of 10^1–10^2 s (Figure S4B). As shown in Figure 3C, the average diameter of AuNPs decreases with the gold ion concentration at a fixed R of 0.06 because a higher degree of supersaturation at a higher gold concentration condition produced smaller gold nuclei during the nucleation process. However, the concentration of 4.8 mM resulted in inhomogeneous deposition (Figure 3B), possibly because of the reaction rate of AuNP seeding, which was faster at this high concentration than the mixing process.

The silica surface state also affects AuNP seeding. We varied the pH values of a mixed suspension of APTS-SiO$_2$ and HAuCl$_4$ to change the zeta potential of the APTS-SiO$_2$ and found that higher pH conditions (smaller zeta potential) produced larger AuNPs (5.8 nm for pH = 4.7 and 7.8 nm for pH = 8.6) on the core silica surface (Figure S5). AuNP deposition could not be confirmed for unmodified bare silica particles with a negative zeta potential. Because the stronger affinity between the core particle surface and gold ions results in more uniform gold-decorated silica particles, these results strongly suggest that AuNP seeding in our microreactor process proceeds *via* heterogeneous nucleation on the solid–liquid interface.

However, the homogeneous nucleation of AuNPs in the bulk solution phase followed by adsorption on the core silica surface cannot be excluded as a possible formation mechanism of the gold-decorated silica particles. We conducted the following control experiment to further investigate the AuNP seeding process. As shown in **Figure 4**A, we first mixed a $HAuCl_4$ solution with a $NaBH_4$ solution in the microreactor to prepare AuNPs through homogeneous nucleation, after which the reaction suspension was mixed with an APTS-SiO_2 suspension in the second microreactor such that the prepared AuNPs were adsorbed onto the core particle surface. The residence time between the first and second microreactors was set to 50 s, which is sufficiently long for the AuNPs to form, as confirmed by the UV-Vis extinction spectra of the homogeneous nucleation process (Figure S4B). As shown in Figure 4B and 4C, this process, consisting of homogeneous nucleation followed by adsorption, produced gold-decorated silica particles with lower coverage. Furthermore, some of the AuNPs remained unattached (indicated by an arrow in Figure 4B and a dotted square in Figure 4C), demonstrating that not all nanoparticles could attach to the core silica surface through the adsorption process.

From results, a mechanism for the gold-decorated silica particles in the flow synthesis process in our microreactor was proposed, as shown in **Figure 5**. Before the reduction reaction, negatively charged gold complex ions are thought to crowd around a positively charged APTS-SiO_2 to form an electric double layer (Figure 5A). Upon mixing with the reducing agent, $NaBH_4$, the reduction of gold ions proceeds based on the supersaturation degree of the reduced gold atoms, which is higher than that of the bulk solution, particularly in the vicinity of the particle surface, thus leading to increased nucleation at the interface. Another factor involved in the mechanism of the gold-decorated silica particles is the electrostatic attraction between the APTS-SiO_2 core and the AuNPs. Because the AuNPs are negatively charged, they are stabilized on the surface of the APTS-SiO_2 to facilitate the heterogeneous nucleation (Figure 5B). The nuclei on the APTS-SiO_2

surface become larger though the diffusion of reduced gold atoms surrounding the APTS-SiO$_2$ particles to complete the formation of the gold-decorated silica particles (Figure 5C). Thus, the reaction period required for AuNP seeding is characterized by the diffusion of reduced gold atoms toward the APTS-SiO$_2$ surface, which means that uniform gold-decorated silica particles would form if the characteristic mixing time to achieve a homogeneous reaction field is shorter than the reaction period characterized by the diffusion of gold atoms. The diffusion time can be easily estimated by dividing the square of the diffusion distance by the diffusion coefficient, assuming that reduced gold atoms travel over, at most, half of the surface distance between core silica particles. For instance, in a silica particle suspension of 2 g/L, the average surface distance between silica particles is 0.9 µm; thus, the diffusion time is calculated to be 0.2 ms when the diffusion coefficient is 10^{-9} m^2/s and the silica density is 2,000 kg/m^3, which are representative values. Thus, the AuNP seeding reaction is expected to be complete in several tenths of a millisecond when using a 2 g/L silica suspension, which is comparable with the mixing time of the microreactor (0.4 ms) at a flow rate of 10 mL/min (Figure 2G). These calculations demonstrate the validity of our proposed mechanism, and intensive mixing with a mixing time faster than the reaction period can produce uniform gold-decorated silica particles in a one-step flow process.

2.2 One-step flow process of gold shell growth

In the shell formation process, gold ions pre-aged with K$_2$CO$_3$ (referred to as K-gold) are reduced in a suspension of as-prepared gold-decorated silica particles to grow AuNP seeds on the silica surface into a contiguous shell. In our preliminary experiments, we first attempted to form the shell with a strong reducing agent, NaBH$_4$, to fully utilize the high mixing performance of the microreactor; however, this attempt was not successful.[29] Seed AuNPs on the silica surface grew larger at higher gold ion concentrations, although newly formed AuNPs were observed in the bulk solution phase at $R = 1.7$ before shell formation was completed (Figure S6). This result suggests that a strong reducing agent is not favorable for

shell growth because the energy barrier to self-nucleation can be easily overcome due to the strong reducing ability. Thus, we used a weaker reducing agent, ascorbic acid (referred to as AA), instead of $NaBH_4$ and used an AA concentration close to a stoichiometric amount. This approach was effective, as the seed AuNPs grew larger without self-nucleation in the bulk phase even at a larger R of 2.5, suggesting that AA favors the growth rather than self-nucleation even though shell formation was not yet completed (**Figure 6**A). Increases in R led the gold islands to grow larger and merge into a complete gold shell at $R = 7$, as shown in Figure 6B. We measured the average shell thickness to be 17 nm by subtracting the core particle diameter from the size of the prepared nanoshell particles. Consider a simple analytical calculation in which a 100% reaction rate is assumed and densities of 18,900 and 2,000 kg/m^3 are used for gold and silica, respectively;[19] this calculation yields a theoretical thickness of 12 nm, which is close to the experimental result, indicating that almost all of the gold ions were consumed in our reaction system. The shell thickness increased linearly with R values up to 50 nm at $R = 20$, as shown in Figure 6C and Figure S7, although a further increase in R resulted in the formation of AuNPs in the bulk solution phase. Figure 6D presents the UV-Vis extinction spectra of the samples with various values of R as well as that of a suspension of gold-decorated silica particles. The spectra peaks shift to longer wavelengths with increasing R values, and the spectrum for $R = 7$ with a peak wavelength of 771 nm agrees well with the theoretical spectrum (dotted line) of a gold nanoshell with a thickness of 14 nm, which was calculated with simulation software based on Mie theory.[30] The XRD spectrum of the gold nanoshell particles with a measured shell thickness of 17 nm (Figure 6E) exhibits sharp peaks corresponding to Au(111) and Au(200), indicating that the prepared shells have a crystalline structure. We calculated a crystal size of 16 nm using Scherrer's equation, which corresponds well with the measured shell thickness. The particle size distribution of a gold nanoshell suspension for $R = 7$, measured using the dynamic light scattering technique, has an average diameter that is 23 nm larger than that of bare silica

particles (Figure S8), indicating that the average shell thickness is 11.5 nm. Figure S8B indicates that no small particles are detected less than 60 nm in the size distribution profile. These results demonstrate that our technique enables the flow synthesis of complete gold nanoshells without self-nucleation in the bulk solution phase using the microreactor. Prepared gold nanoshells are less stable than gold-decorated silica particles and get aggregated in a few days. Addition of surfactants or stabilizing polymers would enhance the suspension stability.

Because we used AA, which has a weaker reducing ability than $NaBH_4$, the reaction rate is assumed to be slower than that with $NaBH_4$, which may lead one to consider whether the microreactor is necessary in the shell formation reaction. However, the use of a Y-shaped mixer instead of the microreactor resulted in a mixed suspension of unreacted particles (gold-decorated silica particles), particles in the process of growing, and gold nanoshells (**Figure 7**A). The batch reaction produced gold nanoshells, but AuNP nucleation was observed (white arrows in Figure 7B), demonstrating that the reaction with AA remained rapid (on the order of a millisecond) (see also Figure 2G). Such a quick reaction demonstrates the need for a microreactor for the synthesis of uniform gold nanoshells under the concentration conditions employed.

To investigate the growth process of gold seeds into a contiguous shell in our synthetic flow system, we used TEM to observe the structural evolution of gold nanostructures on a core silica particle by freeze-drying one drop of a reaction suspension collected on a TEM grid from the outlet with various residence times. In this series of experiments, the concentrations of the reactants were set to be one tenth of our typical concentration set to slow the reaction rate. With the original reaction rate, gold nanoshell formation was completed at the outlet and the growth process could not be traced. The TEM images in Figure S9 demonstrate that as the reaction time increases, gold islands gradually grow and merge with each other, which agrees with the *in situ* measurements of second-harmonic light scattering.[31] This result along with the XRD measurement in Figure 6E

suggests that the structure of gold nanoshells is multicrystalline formed through the fusion of AuNP seeds. Because our synthetic flow process can precisely control the residence time after mixing by varying the tube length and flow rate, our technique is promising for not only the synthesis of gold nanoshells but also the synthesis of silica-gold nanostructures in which the shape and size can be controlled by terminating the reaction at an arbitrary residence time.

2.3 Sequential flow synthesis of gold nanoshells from APTS-SiO$_2$

We next combined the synthetic flow processes for gold-decorated silica particles and gold nanoshells into one sequential process, as shown in **Figure 8**A and Figure S10. In the first microreactor, a mixed suspension of APTS-SiO$_2$ and HAuCl$_4$ was mixed with NaBH$_4$ to produce gold-decorated silica particles, followed by the addition of K-gold in a Y-shaped mixer. The reaction suspension was directly injected into the second microreactor to react with AA. The initial concentrations in the syringes were 0.125 g-silica/L APTS-SiO$_2$ and 0.038 mM HAuCl$_4$, 0.2 mM NaBH$_4$, 2.2 mM K-gold, and 4.0 mM AA, which corresponds to $R = 0.06$ for the AuNP seeding and $R = 7$ for the shell growth process. The residence times between the first microreactor and Y-shaped mixer and between the Y-shaped mixer and second microreactor were set to be 2 and 1 s, respectively, such that they are considerably longer than the characteristic mixing times. The sequential process successfully produced uniform gold nanoshells without the formation of AuNPs in the bulk solution phase, as shown in Figure 8B, C. The TEM image analysis indicated that the shell thickness was 20 nm, which is approximately equal to that obtained from the single shell growth process shown in Figure 6, *i.e.*, within the calculated measurement error in shell thickness. In addition, the UV-Vis extinction spectra of the gold nanoshell suspensions prepared from the single and sequential processes are highly similar, as shown in Figure S11, demonstrating that AuNP seeding and shell growth occurred sequentially in each of the microreactors, as intended.

In our current setting, the total flow rate from the outlet is 60 mL/min, demonstrating the high throughput of our process compared with typical microfluidic systems. A higher flow

rate is possible but depends on the performance of the syringe pumps. In addition, our technique requires no post-synthesis washing steps to remove the free AuNPs, which reduces the time and effort from that required for batch-type synthesis. To the best of our knowledge, this is the first successful attempt for a continuous flow synthesis of gold nanoshells from surface-modified silica particles. Our flow process enables the facile and scalable synthesis of gold nanoshells, which would enable their industrial applications in various fields. Another advantage of our technique is the precise control of the residence time between the reactors (on the order of milliseconds) due to the excellent mixing performance of the microreactor. Setting a residence time between the first and second microreactors that is comparable to or shorter than the formation period of gold-decorated silica particles enables further manipulation of the gold shell thickness and structure by capturing the "intermediate" structures of silica particles decorated with smaller Au seeds and feeding them into the second microreactor, in which the shell growth reaction proceeds. Further studies on this topic are underway.

3. Conclustions

We have demonstrated the flow synthesis of gold nanoshells by applying a non-segmented single-phase microreactor to the AuNP seeding and shell growth processes in the seed-mediated growth method. In the AuNP seeding process, we mixed APTS-SiO$_2$, HAuCl$_4$, and NaBH$_4$ in the microreactor to rapidly reduce the gold ions in the presence of core silica particles and demonstrated that our flow process allows the one-step synthesis of gold-decorated silica particles without the formation of unattached free AuNPs. The high mixing intensity provided by the microreactor is critical to the AuNP seeding process, and the characteristic mixing time (on the order of milliseconds) is required for the uniform deposition of monodispersed AuNPs. In addition, our detailed investigation clarified that the seeding reaction proceeds through heterogeneous nucleation on the surface of the core silica

particles. Thus, the gold-to-silica ratio is a key parameter for increasing heterogeneous nucleation while suppressing nucleation in the bulk solution phase. In the shell growth process, we mixed gold-decorated silica particles, K-gold, and a reducing agent in the microreactor to grow gold seeds in a contiguous shell. We found that a weak reducing agent, ascorbic acid, is suitable for completing the shell formation without preparing free AuNPs in the bulk solution phase, thereby enabling a flow process for shell growth. The shell thickness varies from 17 to 50 nm with variations in the gold-to-silica ratio. The establishment of two separate flow processes for the AuNP seeding and shell growth enabled us to achieve sequential flow synthesis of gold nanoshells directly from APTS-SiO$_2$ by combining these two processes. Because our technique relies on the reaction at the interface, which is a universal phenomenon, we expect our technique to be widely applicable to different combinations of core materials and shell species and to contribute to the development of core-shell material synthesis. However, the sequential flow process established in the present study is still semi-continuous in view of all reactions involved in the seed-mediated growth method because the synthesis of core silica particles and their surface functionalization is not incorporated into the flow system. Establishing the flow sythesis and subsequent functionalization of core particles is required for a complete flow process. We are now working on this topic and will discuss in a future publication.

4. Experimental Section

Materials: An aqueous suspension of silica particles with a diameter of 120 nm (Spherica Slurry 120) was purchased from Catalysts & Chemicals Ind. Co., Ltd. (Japan). The diameter was reported by the manufacturer. 3-Aminopropyl trimethoxysilane (APTS, 97%), L-ascorbic acid (AA, ≥ 99%), chloroauric acid (HAuCl$_4$, 30 wt% solution), potassium carbonate (K$_2$CO$_3$, 99.99%), and sodium borohydride (NaBH$_4$, 99%) were purchased from Aldrich. Ammonium hydroxide (28%), hydrochloric acid (0.1 M), and sodium hydroxide (0.1 M) aqueous solutions

were purchased from Kishida Chemical Co., Ltd. (Japan). All chemicals were used without further purification. All chemicals and the silica particle suspension were diluted to the desired concentration with ultrapure water (resistivity > 18 MΩ·cm) obtained from a water purifier system (Millipore Corp., Bedford, MA).

APTS functionalization on the silica particles: The silica particle surface was modified with APTS to make the surface positively charged, which increases the affinity of the surface to negatively charged gold complex ions and gold nanoparticles. We followed the modification procedure reported by Rasch *et al.*[21] except for the use of water instead of ethanol as the solvent. 0.1 mL of a 28% ammonium hydroxide solution was added to 10 mL of a 1 mg/mL silica suspension under magnetic stirring, followed by the addition of 0.5 mL of a 10% v/v of APTS aqueous solution. The mixed suspension was then stirred for 24 h at 1,500 rpm. The suspension was centrifuged at 3,500 rpm for 1 h to initiate the settlement of the suspended particles, after which the supernatant was discarded and 10 mL of ultrapure water was added to redisperse the particles. This procedure was repeated, and 50 µL of 0.1 mol/L hydrochloric acid was added to the suspension to adjust the pH value to approximately 3. We measured the zeta potential of the silica particles before and after the above-mentioned treatment and confirmed that it became positive (+45 mV) after treatment from the initial −25 mV of the original bare silica particles at pH = 3.2, demonstrating the successful surface modification *via* APTS. The isoelectric point of the APTS-modified silica (APTS-SiO$_2$) particles was measured to be 8.7 (Figure S1A). The zeta potential of the APTS-SiO$_2$ and the pH value of the suspension remained nearly constant for at least one month (Figure S1B).

AuNP seeding on APTS-SiO$_2$: Figure 1 presents a schematic of the experimental setup. An APTS-SiO$_2$ suspension was mixed with a HAuCl$_4$ aqueous solution, and 6 mL of the premixed suspension in syringe A and 6 mL of a NaBH$_4$ aqueous solution in syringe B were injected into the microreactor *via* a two-channel syringe pump. The reduction of the gold ions

proceeded in the presence of core silica particles immediately after mixing, followed by the nucleation of AuNPs. The reaction suspension was collected in a vial through a silicon tube (with an inner diameter of 1.5 mm and a length of 40 cm) connected to the outlet of the microreactor and stirred for 3 min at 1,500 rpm. We used a Y-shaped mixer (with an inner diameter of 1.5 mm) instead of the microreactor with the same flow rate of 10 mL/min to examine the effect of the mixing intensity on the Au seeding. We also conducted a batch-type synthesis in which 10 mL of a $NaBH_4$ solution was added to 10 mL of a premixed suspension of APTS-SiO_2 and $HAuCl_4$ *via* pipette followed by stirring for 3 min at 1,500 rpm.

We varied the core silica particle concentration with a fixed ratio of gold ions to silica particles, R ($\equiv$ Au [g/L]/Silica [g/L]) = 0.06, and a fixed molar ratio of the reducing agent to gold ions, [$NaBH_4$]/[$HAuCl_4$] = 20. A group of typical concentrations after mixing is 0.25 g/L silica particles and 0.075 mM $HAuCl_4$, and 1.5 mM $NaBH_4$. The flow rate of each inlet fluid was set to 10 mL/min (*i.e.*, a total flow rate of 20 mL/min from the outlet) unless otherwise stated. All experiments were conducted at room temperature.

Gold nanoshell formation: The experimental setup is the same as that shown in Figure 1. Gold-decorated silica particles mixed with a K-gold solution in syringe A and a reducing agent solution in syringe B were injected into the microreactor to grow gold seeds attached on the core silica surface. Ascorbic acid was used as the reducing agent. A K-gold solution was prepared as follows. After 0.034 g of K_2CO_3 was dissolved in 15 mL of ultrapure water, 50 μL of a 30 wt% $HAuCl_4$ solution and 10 mL of ultrapure water were added to the solution, and the solution was stirred for 30 min at 1,500 rpm. The solution was then kept in the dark for 24 h. The solution color changed from faint yellow to colorless after stirring, indicating that a ligand exchange reaction of gold(III) complex ions had occurred, replacing Cl$^-$ with OH$^-$. The pH of the solution was approximately 9, and at this pH, the dominant complex species is reported to be [AuCl(OH)$_3$]$^-$.[32] The [AuCl(OH)$_3$]$^-$ complex is less reactive than

$AuCl_4^-$,[33] thereby promoting the growth of Au seeds and suppressing the self-nucleation of gold nanoparticles in the solution phase. To investigate the effect of the mixing intensity on the shell growth process, we used a Y-shaped mixer with an inner diameter of 1.5 mm and a batch reactor using the same procedures as those for the Au seeding process.

We used as-prepared gold-decorated silica particles without washing and investigated the effect of R ($\equiv$ Au [g/L]/Silica [g/L]) on the shell growth reaction with a fixed molar ratio of ascorbic acid to gold ions of 1.8. The typical concentrations of ascorbic acid and gold ions after mixing were 1.0 and 0.54 mM, respectively. The flow rate of each inlet fluid was set to 10 mL/min. All experiments were conducted at room temperature.

Characterization: The extinction spectra of the suspensions of prepared samples were measured with a UV-Vis spectrophotometer (UV-1700, SHIMADZU corp., Japan). The hydrodynamic diameter and zeta potential of the particles were measured with a Zetasizer Nano ZS (Malvern Instruments Ltd., UK). The prepared particles were observed under a transmission electron microscope (TEM; JEM-1010, JEOL Ltd., Japan). Samples for TEM observation were prepared by placing one drop of the suspension on a carbon-coated copper grid, which was then dried under vacuum. The particle size distribution of AuNPs attached to a core silica particle was obtained by counting at least 200 particles from a TEM image. The internal structure of the gold shells was analyzed by powder X-ray diffraction using Cu Kα radiation (XRD; Ultima IV, Rigaku Corp., Japan).

Supporting Information
Supporting Information is available from the Wiley Online Library or from the author.

REFERENCES

[1]   A. Guerrero-Martinez, J. Perez-Juste, L. M. Liz-Marzan, *Adv. Mater.* **2010**, 22, 1182; N. Zhang, S. Liu, Y. J. Xu, *Nanoscale* **2012**, 4, 2227; S. Shaikhutdinov, H. J. Freund, *Adv. Mater.* **2013**, 25, 49; G. Schileo, *Prog. Solid State Chem.* **2013**, 41, 87.

[2]   B. J. Jankiewicz, D. Jamiola, J. Choma, M. Jaroniec, *Adv. Colloid Interface Sci.* **2012**, 170, 28.

[3]   H. Wang, L. Chen, Y. Feng, H. Chen, *Acc. Chem. Res.* **2013**, 46, 1636; J. P. Holgado, F. Ternero, V. M. Gonzalez-delaCruz, A. Caballero, *ACS Catal.* **2013**, 3, 2169; N. Dia, L. Lisnard, Y. Prado, A. Gloter, O. Stephan, F. Brisset, H. Hafez, Z. Saad, C. Mathoniere, L. Catala, T. Mallah, *Inorg. Chem.* **2013**, 52, 10264.

[4]   L. K. Bogart, G. Pourroy, C. J. Murphy, V. Puntes, T. Pellegrino, D. Rosenblum, D. Peer, R. Lévy, *ACS Nano* **2014**, 8, 3107.

[5]   F. Zaera, *Chem. Soc. Rev.* **2013**, 42, 2746.

[6]   X. Xia, D. Chao, X. Qi, Q. Xiong, Y. Zhang, J. Tu, H. Zhang, H. J. Fan, *Nano Lett.* **2013**, 13, 4562.

[7]   K. Ramasamy, M. A. Malik, N. Revaprasadu, P. O'Brien, *Chem. Mater.* **2013**, 25, 3551.

[8]   L. Rouleau, R. Berti, V. W. Ng, C. Matteau-Pelletier, T. Lam, P. Saboural, A. K. Kakkar, F. Lesage, E. Rheaume, J. C. Tardif, *Contrast Media Mol. Imaging* **2013**, 8, 27.

[9]   C. Loo, A. Lowery, N. Halas, J. West, R. Drezek, *Nano Lett.* **2005**, 5, 709.

[10]   Y. Jin, *Acc. Chem. Res.* **2013**, 47, 138.

[11]   R. Huschka, A. Barhoumi, Q. Liu, J. A. Roth, L. Ji, N. J. Halas, *ACS Nano* **2012**, 6, 7681.

[12]   O. Neumann, A. S. Urban, J. Day, S. Lal, P. Nordlander, N. J. Halas, *ACS Nano* **2013**, 7, 42.

[13]   S. J. Oldenburg, R. D. Averitt, S. L. Westcott, N. J. Halas, *Chem. Phys. Lett.* **1998**, 288, 243; S. J. Oldenburg, S. L. Westcott, R. D. Averitt, N. J. Halas, *J. Chem. Phys.* **1999**, 111, 4729.

[14]   D. G. Duff, A. Baiker, P. P. Edwards, *Langmuir* **1993**, 9, 2301.

[15]   S. Park, M. Park, P. Han, S. Lee, *J. Ind. Eng. Chem.* **2007**, 13, 65.

[16]   A. M. Britto-Silva, R. G. Sobral Filho, R. Barbosa-Silva, C. B. Araujo, A. Galembeck, A. G. Brolo, *Langmuir* **2013**, 29, 4366.

[17]   V. G. Pol, A. Gedanken, J. Calderon-Moreno, M. Palchik, A. Slifkin, A. M. Weiss, *Chem. Mater.* **2003**, 15, 1111; W. Dong, Y. Li, D. Niu, Z. Ma, J. Gu, Y. Chen, W. Zhao, X. Liu, C. Liu, J. Shi, *Adv. Mater.* **2011**, 23, 5392; T. C. Damato, C. de Oliveira, R. A. Ando, P. H. Camargo, *Langmuir* **2013**, 29, 1642.

[18]   Y. Kobayashi, Y. Tadaki, D. Nagao, M. Konno, *J. Colloid Interface Sci.* **2005**, 283, 601; N. Phonthammachai, T. J. White, *Langmuir* **2007**, 23, 11421.

[19]   C. Graf, A. van Blaaderen, *Langmuir* **2002**, 18, 524.

[20]   T. Pham, J. B. Jackson, N. J. Halas, T. R. Lee, *Langmuir* **2002**, 18, 4915; X. Xia, Y. Liu, V. Backman, G. A. Ameer, *Nanotechnology* **2006**, 17, 5435; B. E. Brinson, J. B. Lassiter, C. S. Levin, R. Bardhan, N. Mirin, N. J. Halas, *Langmuir* **2008**, 24, 14166.

[21]   M. R. Rasch, K. V. Sokolov, B. A. Korgel, *Langmuir* **2009**, 25, 11777.

[22]   L. Zhang, Y. Xia, *Adv. Mater.* **2014**, 26, 2600.

[23]   S. Marre, K. F. Jensen, *Chem. Soc. Rev.* **2010**, 39, 1183; C. V. Navin, K. S. Krishna, C. S. Theegala, C. S. S. R. Kumar, *Nanotech. Rev.* **2014**, 3, 39.

[24]   S. Duraiswamy, S. A. Khan, *Nano Lett.* **2010**, 10, 3757.

[25]   L. Gomez, M. Arruebo, V. Sebastian, L. Gutierrez, J. Santamaria, *J. Mater. Chem.* **2012**, 22, 21420.

[26]   N. Hassan, V. Cabuil, A. Abou-Hassan, *Angew. Chem., Int. Ed.* **2013**, 52, 1994.

[27]   H. Nagasawa, N. Aoki, K. Mae, *Chem. Eng. Technol.* **2005**, 28, 324; N. Aoki, K. Mae, *Chem. Eng. J.* **2006**, 118, 189.

[28]   J.-M. Commenge, L. Falk, *Chem. Eng. Process.* **2011**, 50, 979.

[29]   S. Watanabe, T. Hiratsuka, Y. Asahi, A. Tanaka, K. Mae, M. T. Miyahara, *J. Soc. Powder Technol, Japan* **2013**, 50, 478.

[30]   O. Peña-Rodríguez, P. P. González Pérez, U. Pal, *Int. J. Spectrosc.* **2011**, 2011, 583743.

[31]   C. Sauerbeck, M. Haderlein, B. Schürer, B. Braunschweig, W. Peukert, R. N. Klupp Taylor, *ACS Nano* **2014**, 8, 3088.

[32]   P. J. Murphy, M. S. LaGrange, *Geochim. Cosmochim. Acta* **1998**, 62, 3515.

[33]   D. Goia, E. Matijević, *Colloids Surf. A* **1999**, 146, 139.
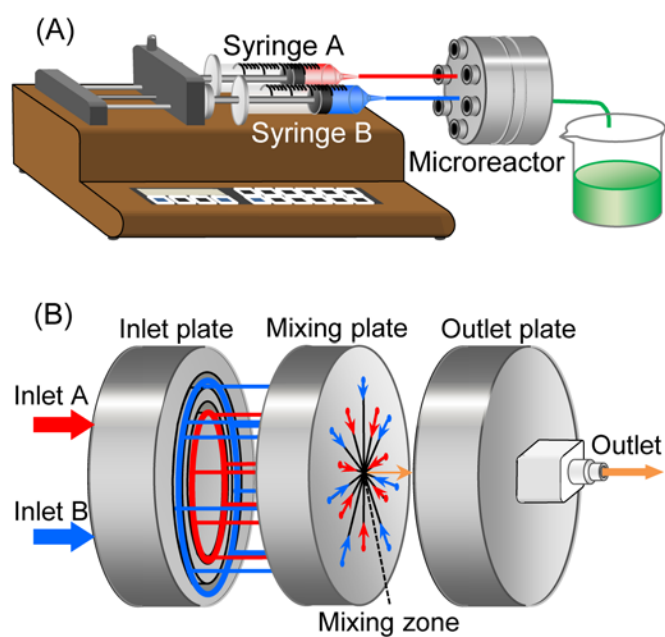
Figure 1. Schematic illustrations of (A) the experimental set-up for the flow synthesis of gold-decorated silica particles and gold nanoshells in the microreactor and (B) the central collision-type microreactor.
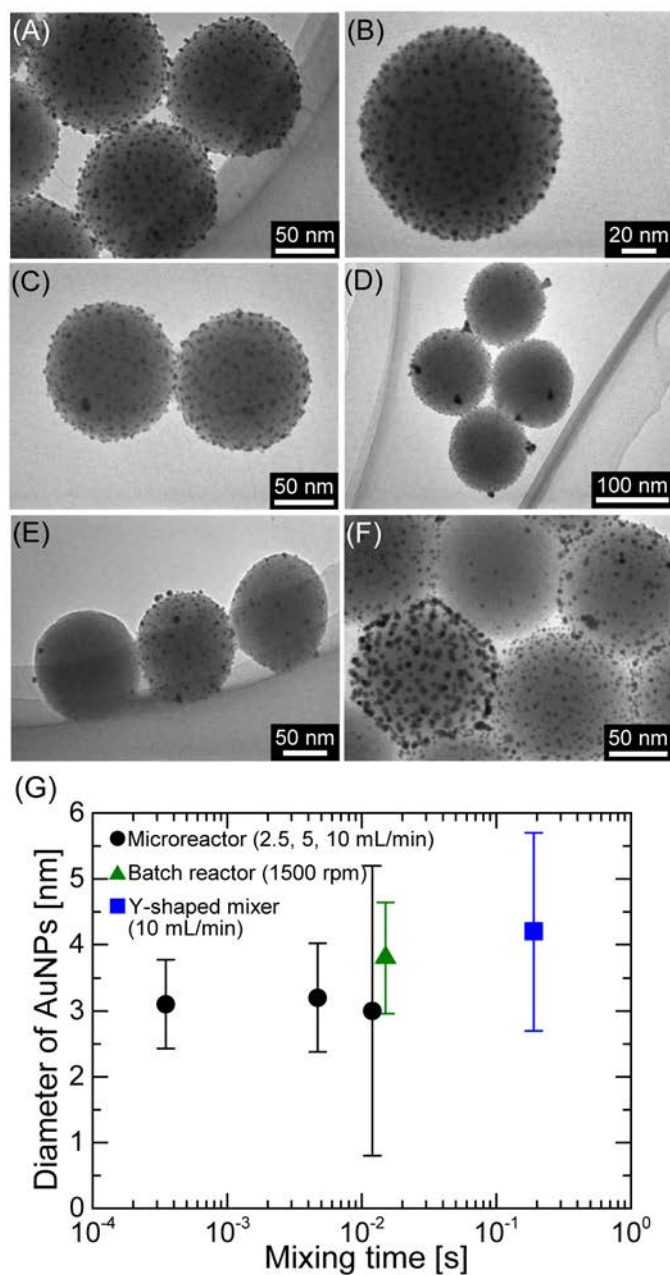
Figure 2. Representative TEM images of gold-decorated silica particles prepared in the microreactor at a flow rate of (A, B) 10 mL/min, (C) 5 mL/min, and (D) 2.5 mL/min, (E) with a batch reactor and (F) with a Y-shaped mixer. (G) Relation between the diameter of the AuNPs attached to core silica particles and the characteristic mixing time.
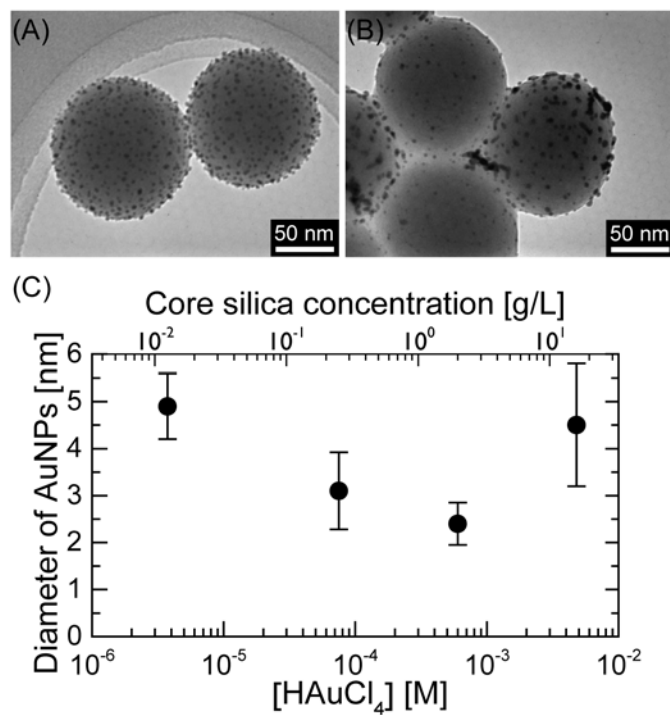
Figure 3. TEM images of gold-decorated silica particles synthesized in the microreactor with a fixed ratio *R* of 0.06 and gold ion concentrations of (A) 0.6 mM and (B) 4.8 mM. (C) Dependence of the AuNP diameter on the gold ion concentration at a fixed ratio *R* of 0.06.
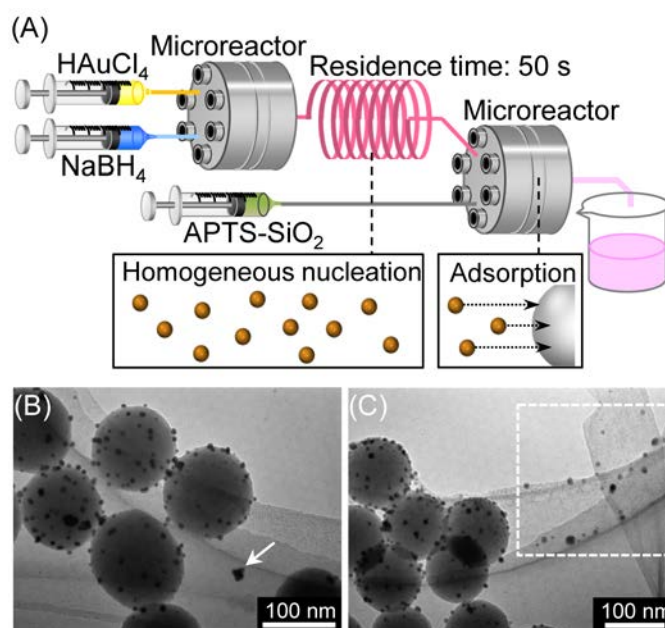
Figure 4. (A) Schematic illustration of the experimental set-up of a control experiment. (B, C) TEM images of the resultant particles. An arrow in (B) and a dotted square in (C) indicate the existence of unattached free AuNPs.
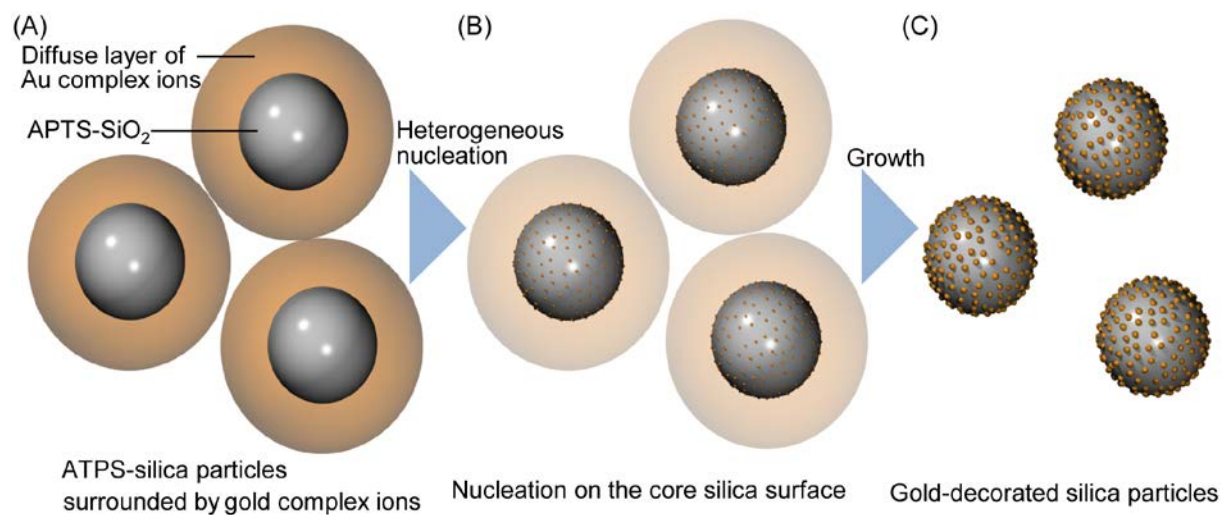
Figure 5. Schematic of a possible formation mechanism of gold-decorated silica particles through the *in situ* reduction of gold ions.
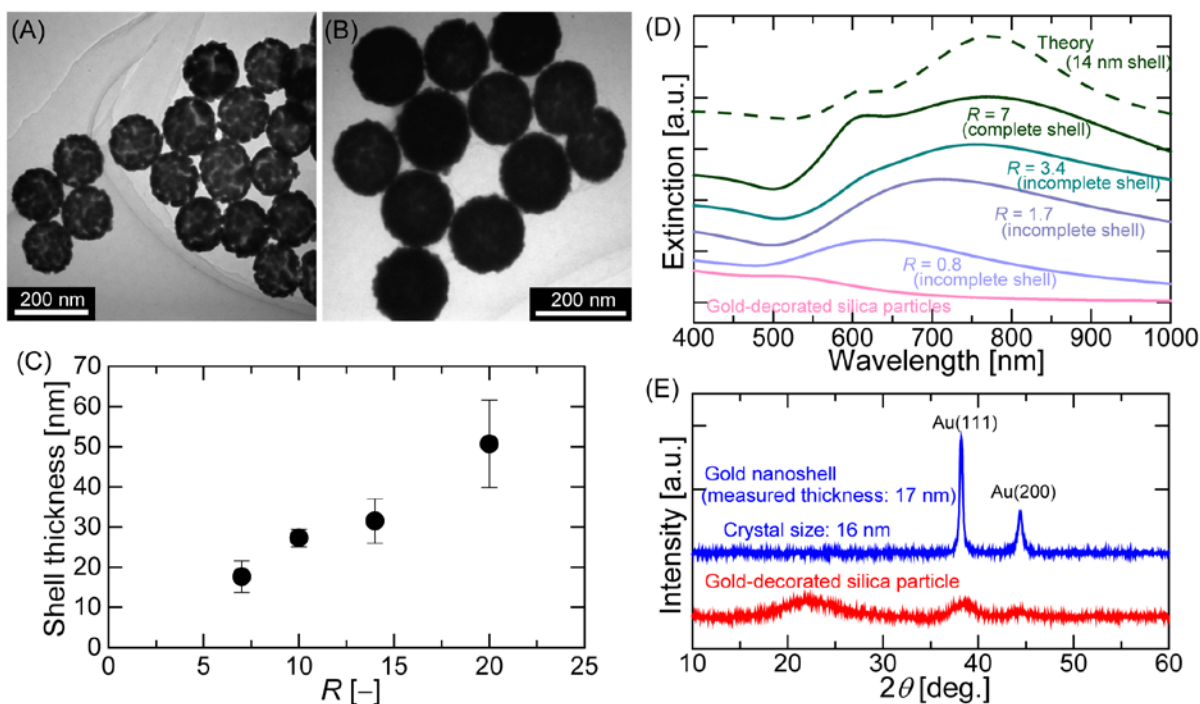
Figure 6. (A) TEM image of silica particles with partially grown gold shell for $R = 2.5$. (B) TEM image of complete gold nanoshell particles for $R = 7$. (C) Relation between the shell thickness and gold-to-silica ratio R. (D) Comparison of the UV-Vis extinction spectra of suspensions before and after the shell growth reaction for different R values with the theoretical calculations for gold nanoshells with a shell thickness of 14 nm. (E) XRD spectra of the gold-decorated silica particles and gold nanoshells with a measured shell thickness of 17 nm.
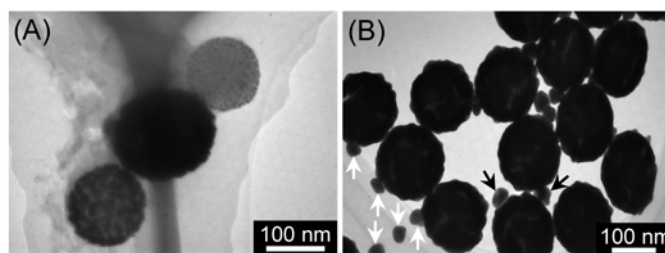
Figure 7. TEM images of the resultant particles after the shell growth reaction for $R = 7$ using (A) a Y-shaped mixer and (B) a batch reactor. Arrows in (B) indicate the formation of AuNPs in the bulk phase.
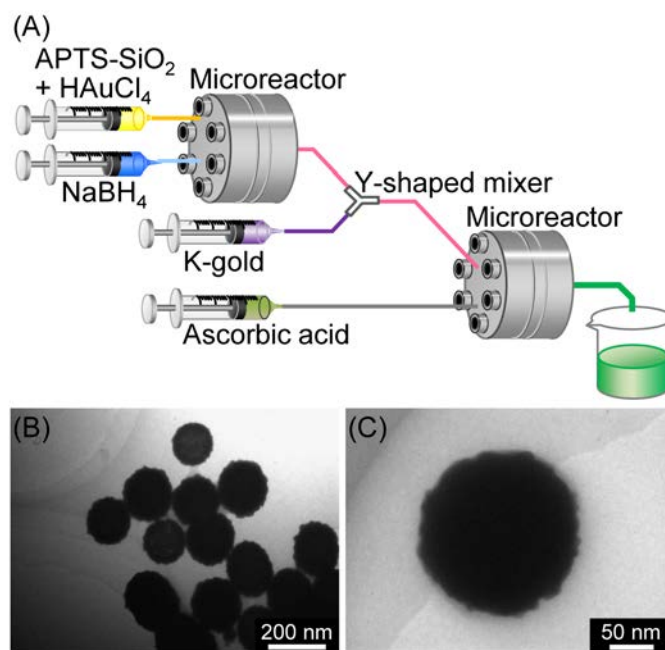
Figure 8. (A) Schematic of the experimental set-up for the sequential flow synthesis of gold nanoshells from APTS-SiO₂. (B, C) TEM images of the resultant gold nanoshells.
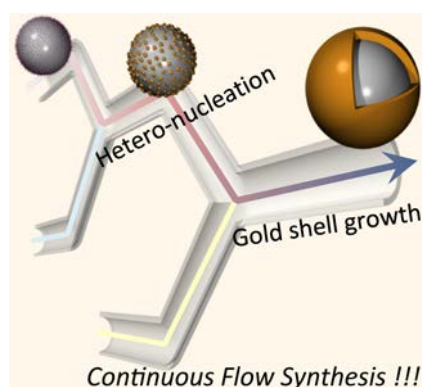
The table of contents entry:

Microfluidic systems are promising for a flow synthetic process of functional nanoparticles. The present study demonstrates that the excellent mixing performance of a non-segmented single-phase microreactor realizes a continuous flow synthesis of plasmonic gold nanoshells through preferential reaction on the core particle surface. The established process is simple, robust and scalable, which would boost their industrial applications in various fields.

Keywords:

Satoshi Watanabe[*], Tatsumasa Hiratsuka, Yusuke Asahi, Asumi Tanaka, Kazuhiro Mae, and Minoru T. Miyahara[*]

Title: Flow Synthesis of Plasmonic Gold Nanoshells via a Microreactor

ToC figure